We are IntechOpen, the world's leading publisher of Open Access books Built by scientists, for scientists

4,800
Open access books available

122,000
International authors and editors

135M
Downloads

Our authors are among the

154
Countries delivered to

TOP 1%
most cited scientists

12.2%
Contributors from top 500 universities

CLARIVATE ANALYTICS BOOK CITATION INDEX INDEXED

WEB OF SCIENCE™

Selection of our books indexed in the Book Citation Index in Web of Science™ Core Collection (BKCI)

Interested in publishing with us?
Contact book.department@intechopen.com

Numbers displayed above are based on latest data collected.
For more information visit www.intechopen.com

8

Mechanical Behavior of Filled Thermoplastic Polymers

S. Bazhenov
Institute of Synthetic Polymeric Materials
Russian Academy of Sciences, Moscow
Russia

1. Introduction

Filled composites consist of a continuous matrix phase and of filler particles [1, 2]. There were three stages in their development. The first one started in late 1950s and was related to the development of solid rocket fuel which contained about 80% of rigid powder particles bonded by an elastic rubber matrix. The second stage began in 1970s with the development of composites based on thermoplastic polymers filled with rigid nonorganic particles. Fracture of these composites is essentially different from that of the rubber matrix composites. The third stage started in late 1980s with the creation of nanocomposites. Nanocomposites are not discussed here, but some mechanisms typical of composites filled by microparticles can be applied to them.

Rigid nonorganic particles are introduced into thermoplastic polymers mainly in order to increase the Young modulus of the material. Sometimes it is done to improve thermal resistance, electric conductivity, magnetic properties, to lower friction wear, flammability and so on [1, 2].

The main disadvantage of filled thermoplastic composites is their brittleness leading to a dramatic decrease in fracture strain in comparison with unfilled polymers [2-5]. An important goal is development of filled polymer composites remaining ductile at high filler contents. The goal of the review is to describe approaches to suppress brittle fracture of thermoplastics filled with particles.

2. Deformation mechanisms

If a polymer yields with necking, an increase in filler content leads to fracture during neck propagation, to quasibrittle fracture during formation of a neck and, finally, to true brittle fracture as illustrated by Fig. 1. At brittle and quasibrittle fracture modes fracture strain is roughly 100-fold lower than that of the unfilled polymer. In addition, filler may suppress necking and initiate yielding in craze-like zones if the bonding with a polymer is weak [6]. Thus, in filled polymers at least six modes of deformation behavior are distinguished: 1) brittle, 2) quasibrittle fracture during neck formation, 3) fracture during neck propagation, 4) stable neck propagation, 5) microuniform yielding, and 6) yielding in crazes [7].

The load versus elongation curve has specific features at each fracture mode (Fig. 2). A typical stress-strain curve of a necking polymer is characterized by the presence of a

maximum. After reaching the yield point, the stress drops and remains constant while the neck propagates through the specimen. This is followed by a region of strain-hardening where the stress gradually increases. Quasibrittle composites reach a stress maximum, however, just past the yield point, as the stress decreases toward the draw stress, composite fractures. In brittle materials the stress-strain relationship is linear and the fracture strain is less then 2-3%. A curve with nonlinear monotonously increasing stress is typical for both uniform yielding and yielding in crazes.

Composites based on polymers with uniform yielding and those deforming by neck propagation behave differently. In polymers deforming without necking (rubber, polytetrafluorethylene or super high molecular weight polyethylene) fracture strain gradually decreases with an increase in filler content but the material remains ductile up to very high filler contents [7,8]. This behavior is different from that of composites based on matrices deforming by neck propagation [3]. Therefore behavior of composites based on matrices deforming uniformly and with necking will be discussed separately.

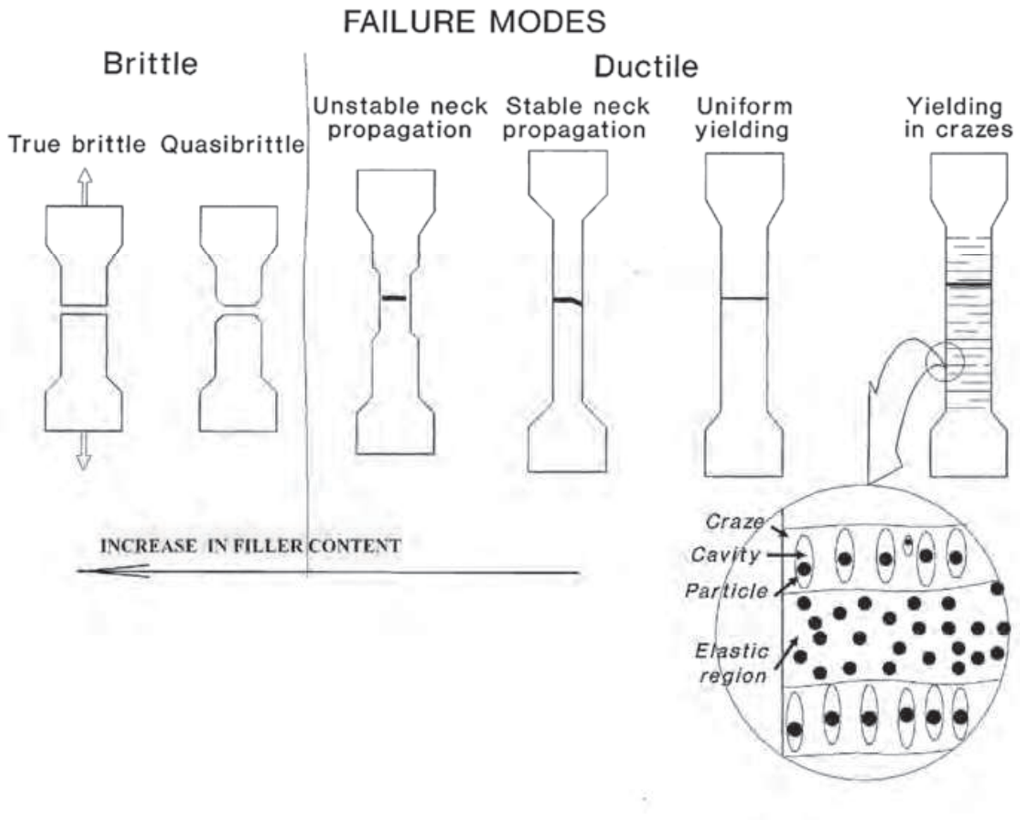

Fig. 1. Fracture modes of filled polymers.

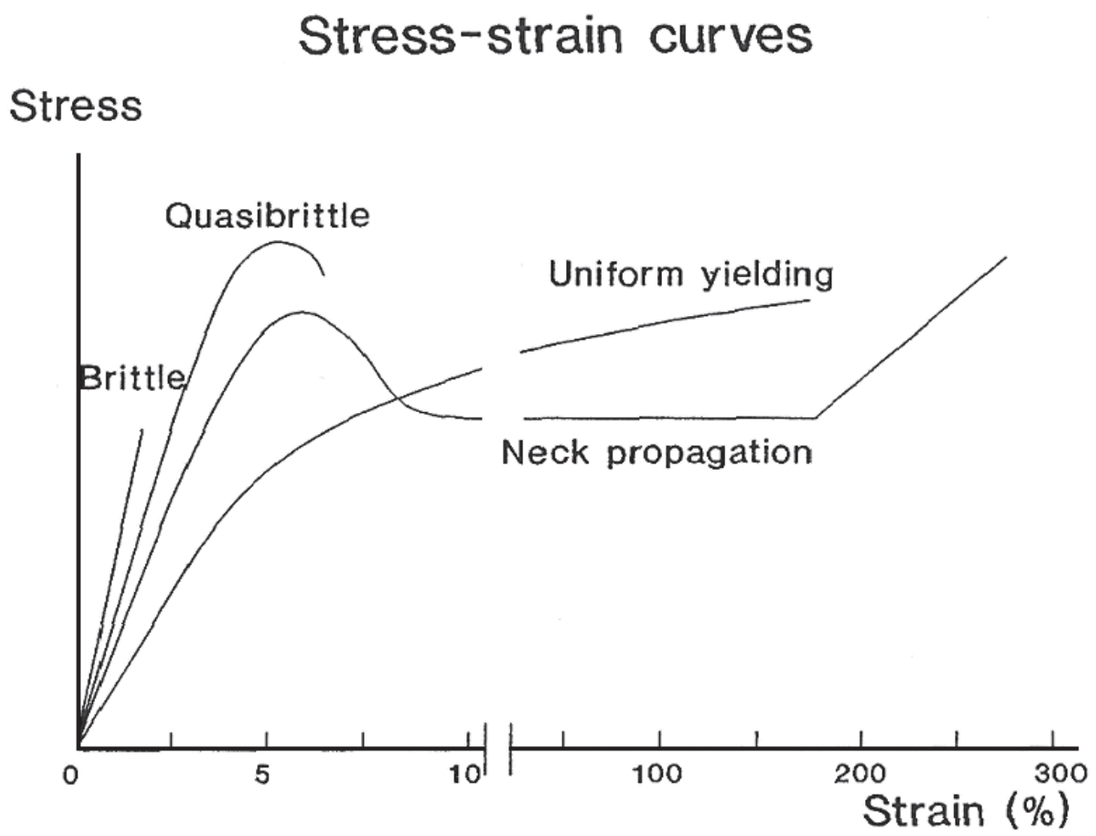

Fig. 2. Typical engineering stress versus strain curves at different fracture modes [5].

3. Deformation at fracture

3.1 Uniform matrix yielding

In polytetraphluorethylene (PTFE) and super high molecular weight polyethylene (SHMWPE) in tension the neck does not appear [7,8]. Both polymers have very high molecular weight and considerable strain strengthening which prevents necking. Due to very high molecular weight their viscosity is high even at elevated temperatures. As a result, they cannot be filled with particles by a traditional liquid technologies. However, SHMWPE was filled by in situ polymerization. A catalyst was put on aluminum particles and the matrix was polymerized [9-11].

Fig. 3 shows typical engineering stress σ - strain ε curves for unfilled SHMWPE and that filled with aluminum particles [8]. The stress-strain curve of unfilled SHMWPE is typical for ductile polymers. The stress gradually increases with an increase in strain. The unfilled polymer reached an engineering strain of approximately 270% before it fractured. The stress-strain curves of the SHMWPE filled with 57 vol.% of particles are similar to that of the unfilled polymer. The fracture strain decreases with an increase in the filler content. However, the fracture strain even at 57 vol.% of Al particles is approximately 100% and the composite remains ductile.

Qualitatively different behavior is observed at the filler content of 62 vol.% (curve 7) when in the material appear pores. These composites reach a yield point on the stress-strain curve,

however, just in the yield point, the specimens fractured at the strain of approximately 2%. The large decrease in fracture strain between 57 and 62 vol.% is typical for the transition from ductile to brittle fracture.

Fig. 4 shows the relative fracture strain $\varepsilon_c/\varepsilon_0$ of filled SHMWPE (1) and PTFE (2) plotted against the volume fraction of particles V_f. Both composites remain plastic up to very high filler contents. Embrittlement of SHMWPE is observed at filler content of 62 vol.%. The decrease of fracture strain at lower filler content is moderate, and both composites remain ductile even at very high filler contents. Thus, embrittlement is not typical for polymers deforming without necking [8].

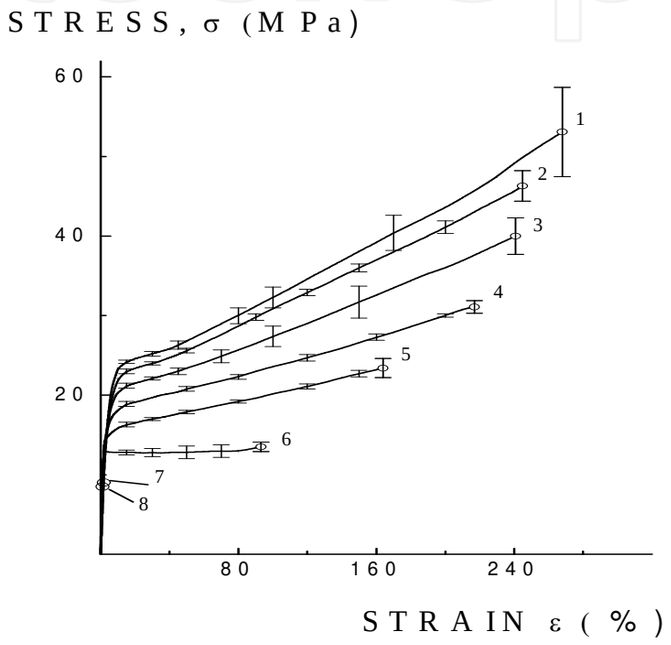

Fig. 3. Typical engineering stress σ versus strain ε curves for unfilled SHMWPE (curve 1) and SHMWPE filled with V = 4 (curve 2), 10 (3), 19 (4), 32 (5), 57 (6) 62 (7) and 63 vol.% (8) of spherical aluminum particles. The diameter of Al particles is ≈10 μm.

3.2 Matrices deforming by neck propagation

Fig. 5 shows typical engineering stress σ - strain ε curves for unfilled PETG and PETG filled with $CaCO_3$ [5] The character of the curves changes with an increase in the filler content. The stress - strain curve of unfilled PETG is typical of ductile polymers. After reaching the yield point, the stress dropped to the draw stress (σ_d) and remained constant while the neck propagated through the entire gauge length of the specimen. This was followed by a region of strain-hardening where the stress gradually increased as the necked material extended uniformly. The unfilled polymer reached an engineering strain of approximately 260% before it fractured. The stress-strain curves of the filled materials with the amount of $CaCO_3$, 2.4 and 7.2 vol.%, were similar to that of the unfilled polymer. However, the fracture strain decreased as the filler content increased and the length of the strain-hardening region also decreased until with 7.2 vol.% there was no strain-hardening. Different behavior was observed with higher filler contents, 14 and 24 vol.%. These compositions also reached a

yield maximum in the stress-strain curve, however, just past the yield point, as the engineering stress was decreasing toward the draw stress σ_d, the specimens fractured. As a result, the fracture strain was in the range of 3-8% which is typical for brittle polymers. The drop in fracture strain between 7.2 and 14 vol.% was caused by the transition was from ductile to quasibrittle fracture.

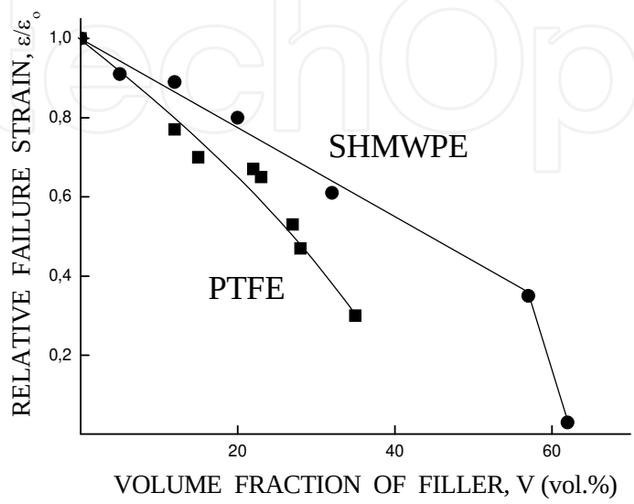

Fig. 4. Relative fracture strain $\varepsilon_c/\varepsilon_0$ of filled SHMWPE (1) and PTFE (2) plotted against the volume fraction of particles V. ε_0 – fracture strain of unfilled polymer. SHMWPE and PTFE are filled with Al and Cu particles respectively. The diameter of particles is $\approx$10 μm.

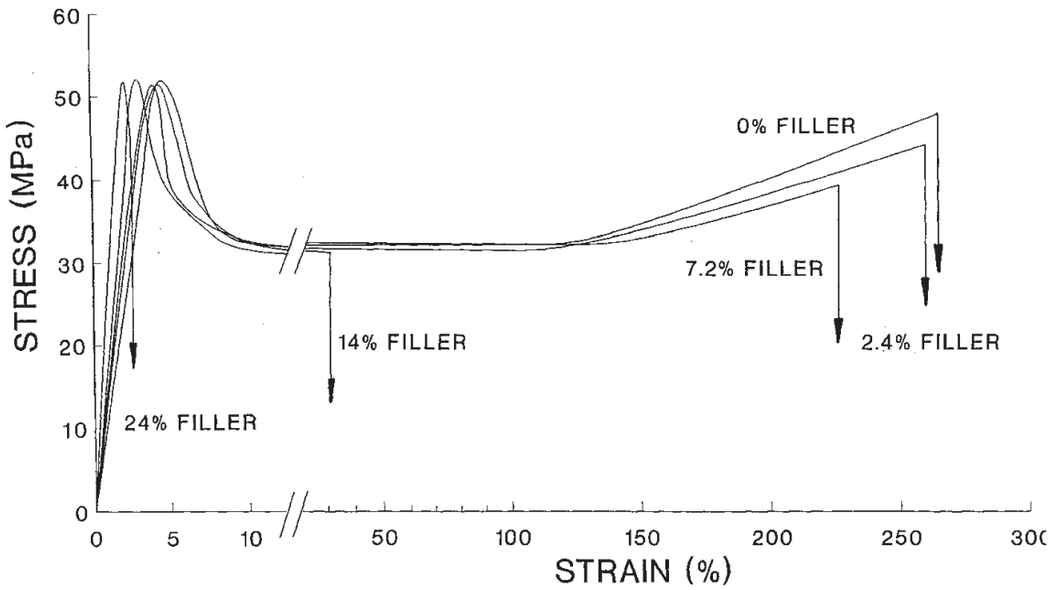

Fig. 5. Typical engineering stress σ - strain ε curves for unfilled PETG and PETG filled with $CaCO_3$ particles.

Photographs of two fractured specimens, one with 2.4 vol.% filler and the other with 14 vol.%, are shown in Fig. 6. The specimen with 2.4 vol.% filler fractured after the neck propagated through the entire gauge section. In contrast, the specimen with 14 vol.% filler showed only localized thinning at the fracture zone while the remainder of the gauge section was not plastically deformed. Necking initiated in both specimens, while the subsequent stability of the neck defined the transition from ductile to quasibrittle behavior. With the lower filler content, the neck was stable and propagated through the gauge length. At the higher filler contents, the neck formed but it was not strong enough to support the drawing, and fracture occurred in the neck. The ductile-to-quasibrittle transition was from propagation of a stable neck through the entire gauge length of the specimen to fracture in the neck without propagation.

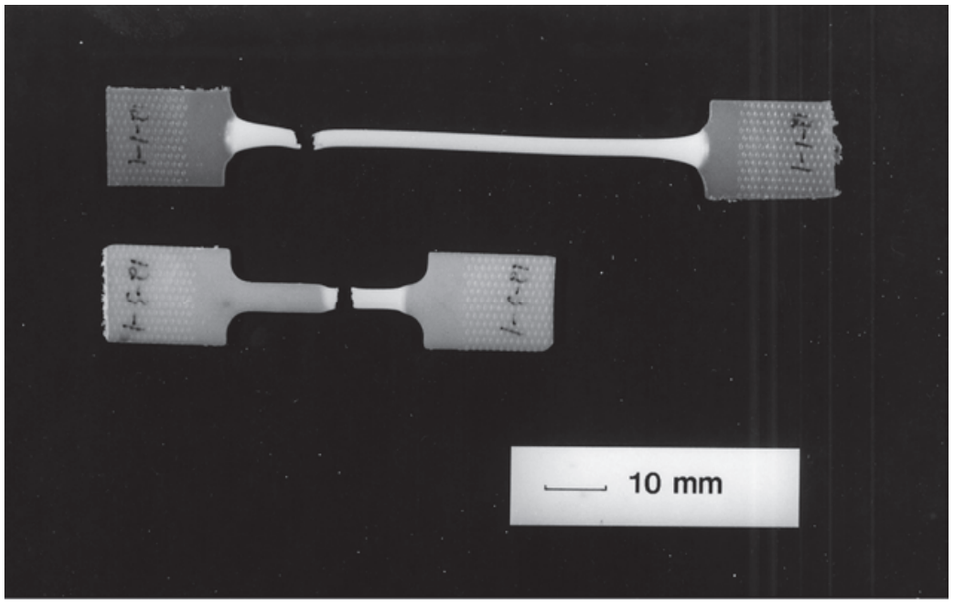

Fig. 6. Photographs of two fractured PETG specimens, one with 2.4 vol.% filler and the other with 14 vol.% of $CaCO_3$ particles.

Fig. 7 demonstrates the effect of particles on relative fracture strain $\varepsilon_c/\varepsilon_0$ of PVC, PET, HDPE and PP. All these polymers yield by neck propagation. The fracture strain depends on the polymer matrix. Most typical dependence is a step-like, and a moderate reduction in fracture strain at low filler contents, similar to that in Fig. 4, is followed by a sharp drop of fracture strain in a comparatively narrow interval of filler contents. The magnitude of strain decrease is approximately 100-fold. The drop in fracture strain is caused by the transition from a ductile to quasibrittle fracture [7].

Fig. 8 illustrates the mechanism of quasibrittle fracture of filled composite. The yielding of the matrix after necking is heterogeneous and localized in the narrow transition zone between the neck and the undeformed part of the sample. The local deformation in the forming neck can reach hundreds of percent. However, if the necking region is not strong enough the neck is not able to propagate along the sample. The length of the forming neck is short, and almost the entire sample is elastic everywhere except the neck zone. If the sample fractures in the forming neck, the average fracture strain is close to the strain of the elastic regions.

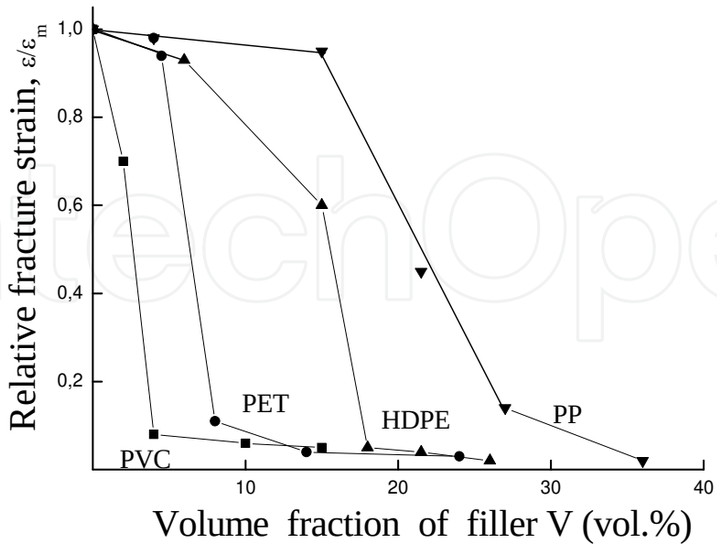

Fig. 7. Relative fracture strain of filled polymers, $\varepsilon_c/\varepsilon_m$ versus the volume fraction of particles V. ε_m - fracture strain of unfilled polymer. (▼) - PP/Al(OH)$_3$, 10 μm; (▲)- HDPE/Al(OH)$_3$, 10 ▲μm; (●) - PET/$CaCO_3$, 8 μm.

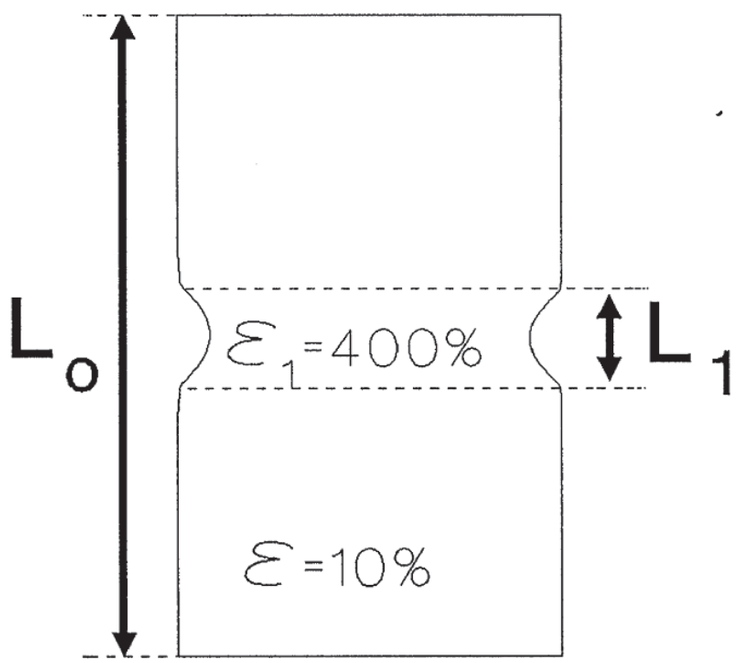

Fig. 8. Schematic of localized yielding of polymer in the narrow transition zone between the neck and the undeformed part of the sample. The local deformation in the forming neck in PP reaches 400% and the rest of sample is elastic. The length of the yield zone L_1 is short, and the composite is elastic on macroscopic scale.

Increase in filler content leads to a decrease in fracture strain in the forming neck as shown in Fig. 4. At low filler contents V this strain is higher than the strain in necking region. As a result, neck propagates through the sample and filled polymer is ductile. However, the composite fracture strain at some critical filler content becomes lower than the strain in the necking region, and the neck does not propagate through the sample. Transition to brittle fracture is accompanied by an approximately 100-fold decrease in the macroscopic fracture strain compared to that of the unfilled matrix. Thus, the material is macroscopically brittle despite local yielding in the forming neck. Hence, the composite on macrolevel is brittle, while on the microlevel in the fracture region it yields.

The neck is not able to propagate along the sample if the engineering draw stress σ_d is higher than the fracture stress. In the transitional point the composite strength is equal to its draw stress. Hence, the criterion of the transition from neck propagation to brittle fracture is described by equation [5]:

$$\sigma_d = \sigma_c \tag{1}$$

where σ_d is the draw stress and σ_c is fracture stress of filled polymer. On this reason below the effect of the particle content V on the draw stress σ_d and the strength σ_c is described.

4. Tensile strength

Fig. 9 shows the effect of particles on the relative strength of various polymers filled with inorganic particles [4]. Relative strength is comparatively insensitive to polymer type and its adhesion to particles. It depends only on the volume fraction of the particles V. This is explained by debonding of the particles in necking region both at week and strong adhesion (Fig. 10).

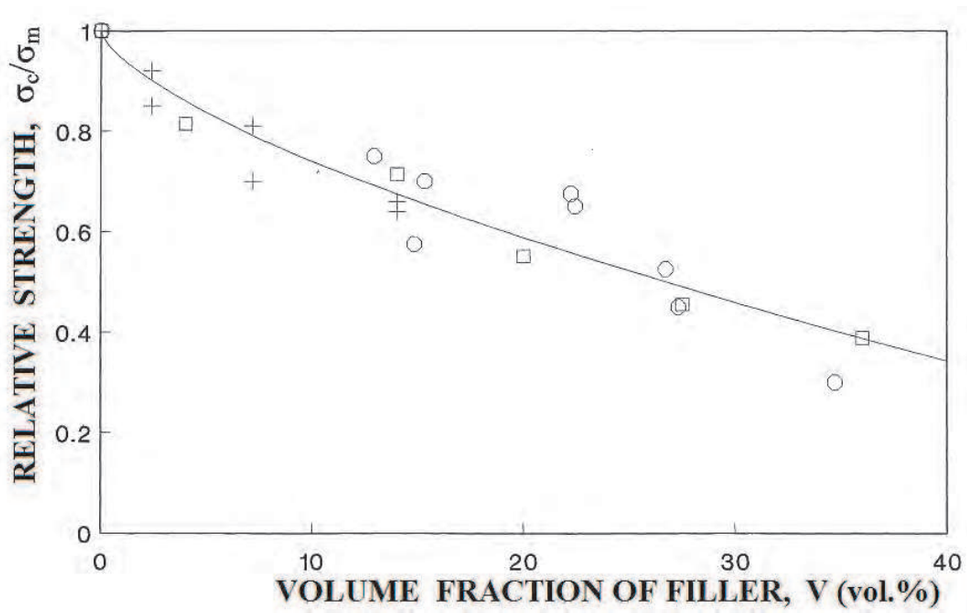

Fig. 9. Relative strength of filled polymer, σ_c/σ_m, versus the volume fraction of particles V. σ_m - strength of unfilled polymer. (o) - PTFE; (+) - PET/$CaCO_3$, diameter of particles 8 μm; (□) - HDPE/$Al(OH)_3$, 1 μm; (x) - HDPE/$Al(OH)_3$, 25 μm [7].

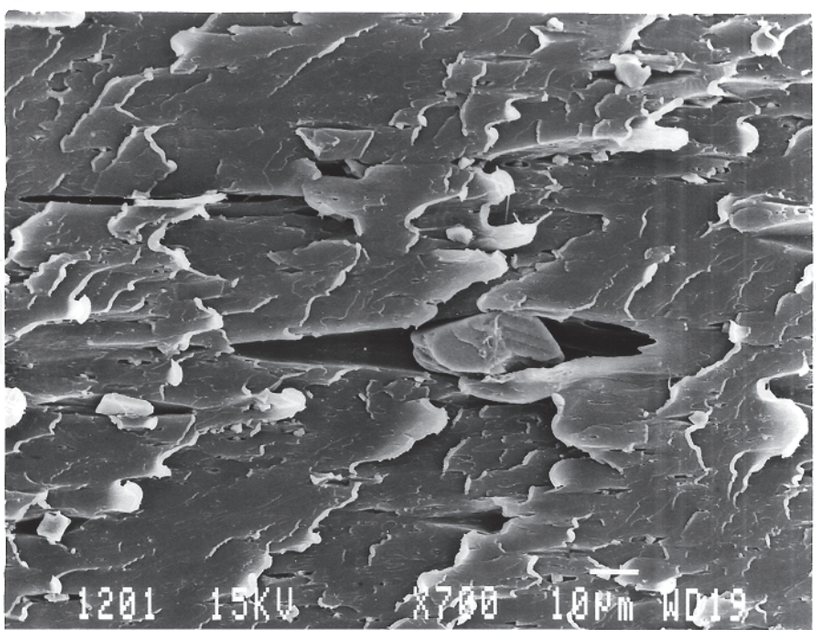

Fig. 10. Debonding of the well-bonded $CaCO_3$ particles from PETG matrix in neck. The sample was tensioned in the horizontal direction [5].

A number of attempts have been made to describe the effect of rigid filler particles on fracture stress and strain analytically. Smith introduced a model in which the composite was modeled by a cubic array of spherical particles [13] (Fig. 11a). He assumed that all particles debond from the matrix prior to fracture so that the crack grows through a plane weakened by the appearing pores (plane AA in Fig. 11). Neglecting stress concentration and assuming

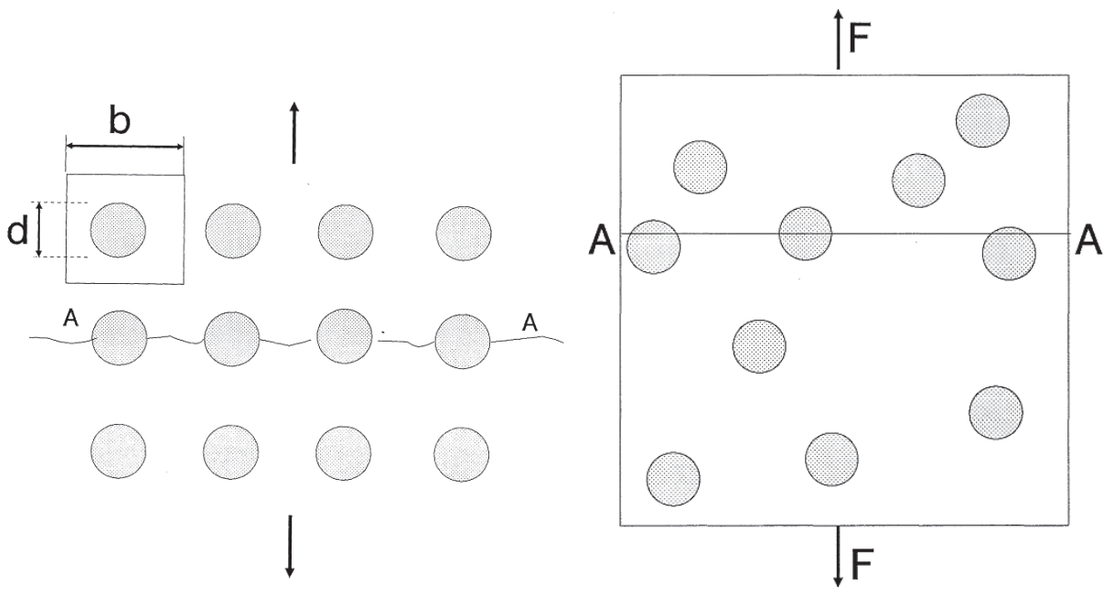

(a) (b)

Fig. 11. Model of regular array (a) and random array of spherical particles [8].

that the strength of the composite is proportional to the cross-section of the matrix in the crack plane AA, the strength is given by equation:

$$\sigma_c = \sigma_m \left(1 - \beta V^{2/3}\right), \tag{2}$$

where β = 1.21. For cubic particles Nielsen derived similar equation with β = 1 [14]. The coefficient β is sometimes called the shape factor. According to equation (2) the strength decreases with an increase in filler content. For example, the strength decrease at V = 40 vol.% is approximately threefold.
For the random particle distribution model (Fig. 11b) the following equation was derived [8]:

$$\sigma_c = \sigma_o \frac{1 - V^{1/3}}{\sqrt{1 + V^{1/3} + V^{2/3}}} \exp\left\{\sqrt{3}\left[\operatorname{arctg}\left(\frac{1 + 2V^{1/3}}{\sqrt{3}}\right) - \frac{\pi}{6}\right]\right\} \tag{3}$$

Expanding equation (3) in series by degrees of $V^{1/3}$, at low filler contents ($V^{1/3} << 1$) it is simplified:

$$\sigma_c = \sigma_m \left(1 - \frac{3}{2} V^{2/3}\right) \tag{4}$$

Fig. 12 shows the strength σ_c of filled SHMWPE plotted against aluminum particles V [8]. Equation (3) describes the strength of the composite (points) in the entire range of filling contents. Curve 1, corresponding to equation (2), describes experimental data only at V < 30 vol.%. Hence, the coefficient β = 1,21 is a fitting parameter adequately describing the experiment at filler contents V < 30 vol.%.

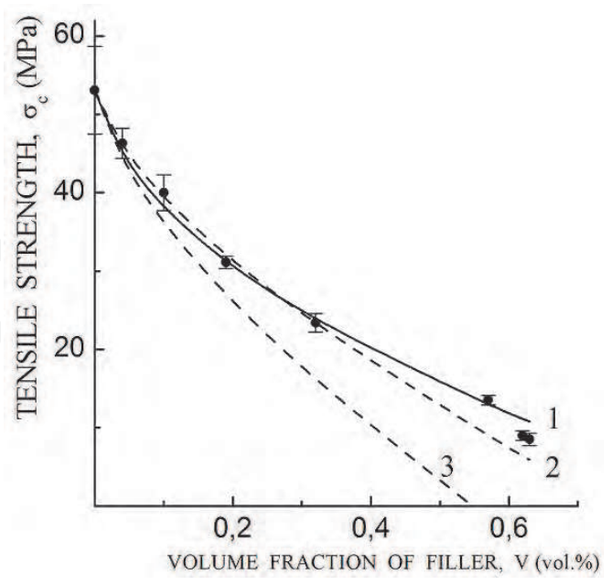

Fig. 12. Comparison of tensile strength σ_c of SHMWPE filled with Al particles. Theoretical values of strength in curves 1, 2 and 3 were calculated with equations (3), (2) and (4) respectively.

5. Draw stress

Fig. 13 shows the relative engineering draw stress σ_c of different filled polymers plotted against the filler content V [7]. In contrast to strength, the draw stress decreases linearly with an increase in the filler content V. The effects of filler on the strength and the draw stress of composite are functionally different. The draw stress depends on adhesion between the polymer and the particles. It is within the dashed fork region depending on adhesion between the polymer and the particles. The upper border of the fork, corresponding to well-bonded particles, is a constant equal to the draw stress of unfilled polymer. The lower border of the fork, corresponding to completely debonded in the yield point particles, is a straight line with the slope approximately equal to minus one. If particles are debonded partially, the draw stress is given by:

$$\sigma_d / \sigma_{dm} = 1 - \alpha V \tag{5}$$

where σ_{dm} is draw stress of unfilled matrix and α is fraction of debonded particles. If adhesion is good and particles are not debonded, α = 0 and equation (5) gives $\sigma_d = \sigma_{dm}$. If all particles are debonded, α = 1 [7].

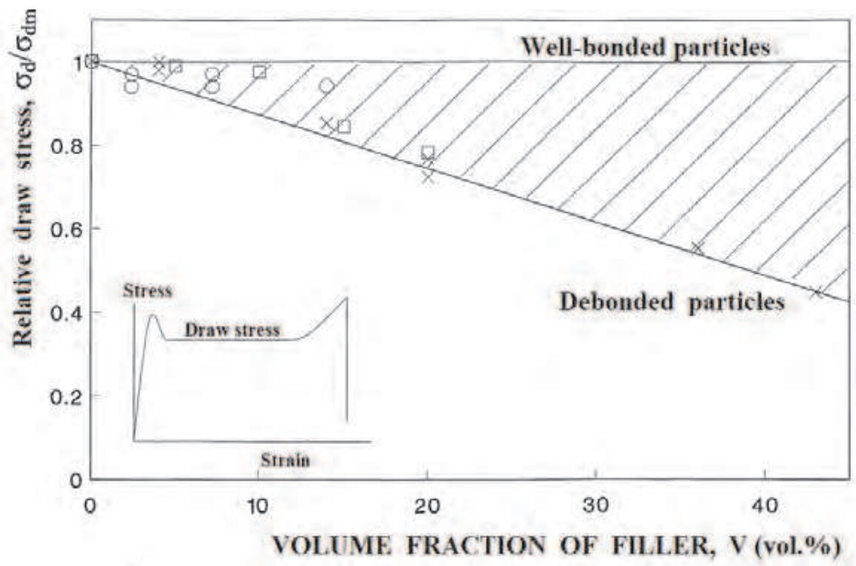

Fig. 13. Relative engineering draw stress of filled polymer, σ_d/σ_{dm}, versus the volume fraction of particles V. σ_{dm} – draw stress of unfilled polymer. (□) - PET/$CaCO_3$, 8 μm; (x) - PP/$Al(OH)_3$, 10 μm; (◊) - HDPE/$Al(OH)_3$, 1 and 25 μm [7].

6. The yield stress

Fig. 14 shows the effect of particles on the relative yield stress σ_y of filled polymers. The yield stress is within the dashed fork region depending on adhesion between the polymer and the particles. The upper border of the fork is a constant equal to the yield stress of the unfilled polymer σ_{ym}. The yield stress of filled polymer is equal to that of unfilled polymer if adhesion is strong and in the yield point particles are well-bonded with the polymer matrix. Reduction of adhesion leads to a decrease in the yield stress. The yield stress is described by

the lower border of the fork if all particles debond before the yield point. If debonding is partial, the yield stress is inside the fork region, and is given by the equation [15]:

$$\sigma_y / \sigma_{ym} = 1 - 1{,}21\alpha V^{2/3} \tag{6}$$

where σ_{ym} is the yield stress of unfilled matrix and α is fraction of debonded particles. If the adhesion between particles and the matrix is high, the particles in the yield point are not debonded, α = 0 and $\sigma_y = \sigma_{ym}$ [3, 16].

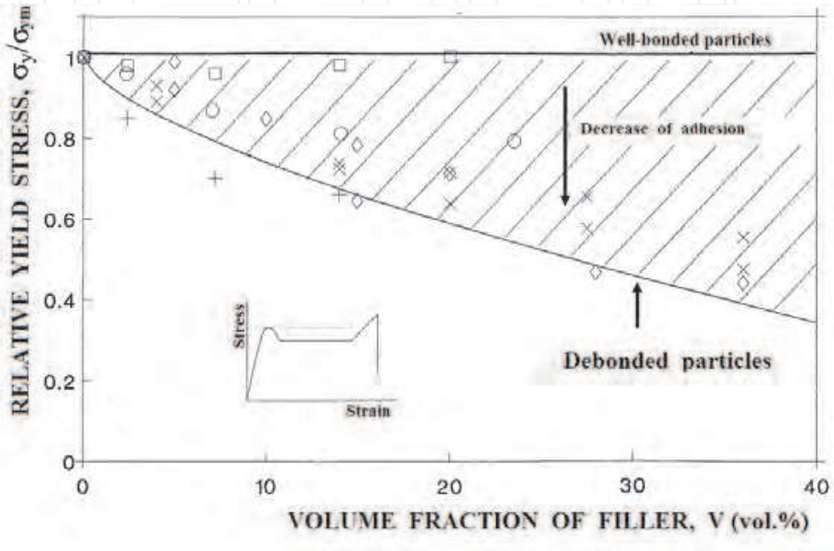

Fig. 14. Relative yield stress of filled polymer, σ_y/σ_{ym}, versus the volume fraction of particles V. σ_{dm} – draw stress of unfilled polymer. (□) - PET/$CaCO_3$, 8 μm [5]; (○) – PET filled with coated $CaCO_3$ particles; (x) - PP/$Al(OH)_3$, 1 and 25 μm; (◊) - HDPE/$Al(OH)_3$, 10 μm [7].

6.1 Transition to brittle fracture

6.1.1 Good adhesion

Fig. 15 shows schematically the composite strength and the draw stress plotted against the filler content V. The composite strength and the draw stress for well-bonded particles were calculated with equations (2) and (5). If the unfilled polymer yields with necking, at low filler contents the strength is higher than the draw stress. As a result, the neck propagates through the specimen, and filler does not change the deformation mode of the polymer. In contrast, at high filler contents the strength is lower than the draw stress, and the neck is not able to propagate through the sample. As a result, the composite fails during neck formation and a ductile-to-brittle transition is observed. The criterion of the transition from neck propagation to brittle fracture is calculated from equations (1), (2) and (5) at α = 0 [5]:

$$V^* = \left(\frac{\sigma_m - \sigma_{dm}}{1.21\sigma_{dm}} \right)^{2/3} \tag{7}$$

where σ_m and σ_{dm} are the strength and the draw stress of the unfilled polymer.

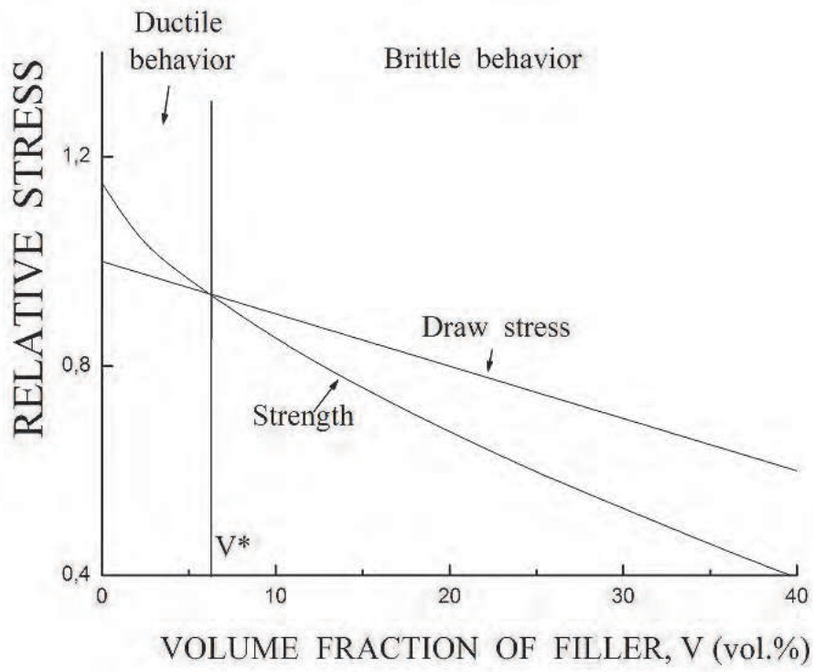

Fig. 15. Schematical drawing of the strength and draw stress of filled polymer plotted against the filler content, V. V* - the critical filler content of the transition from neck propagation to quasibrittle fracture.

Fig. 16 shows the embrittlement filler content V* plotted against the ratio of the strength to the draw stress σ_m/σ_{dm} of unfilled matrix. The critical filler content V* increases with an increase in the ratio σ_m/σ_{dm}. For example, the critical volume fraction V* for polyvinylchloride (PVC) is less than 0.05, and is not improved by toughening with rubber particles. If a polymer does not strain-harden, like PVC, even a small amount of filler leads to loss of composite ductility. The critical volume fractions for PP and for copolymer of ethyleneterephtalate (PET) are higher, from 0.1 to 0.2. The critical filler content of HDPE is from 0.2 to 0.25 and depends on particle size [2]. In general, the ratio σ_m/σ_{dm} describes the ability of the polymer to strain-hardening and hence the critical filler content V* increases with the polymer ability to strain-harden. The critical filler content calculated from equation (7) is plotted as a solid line in Fig. 16. The theoretical curve corresponds to experimental data for different matrices [7].

The polymer strain-hardening rises with an increase in polymer molecular weight. Hence the polymers with high molecular weight become brittle at higher filler contents then that with lower molecular weight. Unfortunately high molecular weight polymers have too high viscosity and are hardly mixable with rigid particles. Thus, requirements of high mechanical properties of composite contradict technological polymer viscosity requirements.

6.2 Weak adhesion

It is generally considered that a composite may have high mechanical properties only at good adhesion of the strengthening phase to a matrix. The example is fiber-reinforced plastics. However, filled composites are exclusion and week particle adhesion may suppress brittle fracture. At weak adhesion filler particles debond from the matrix before the yield

point, and the yield and draw stresses are described by lower boundaries of the forks in Figs. 13 and 14.

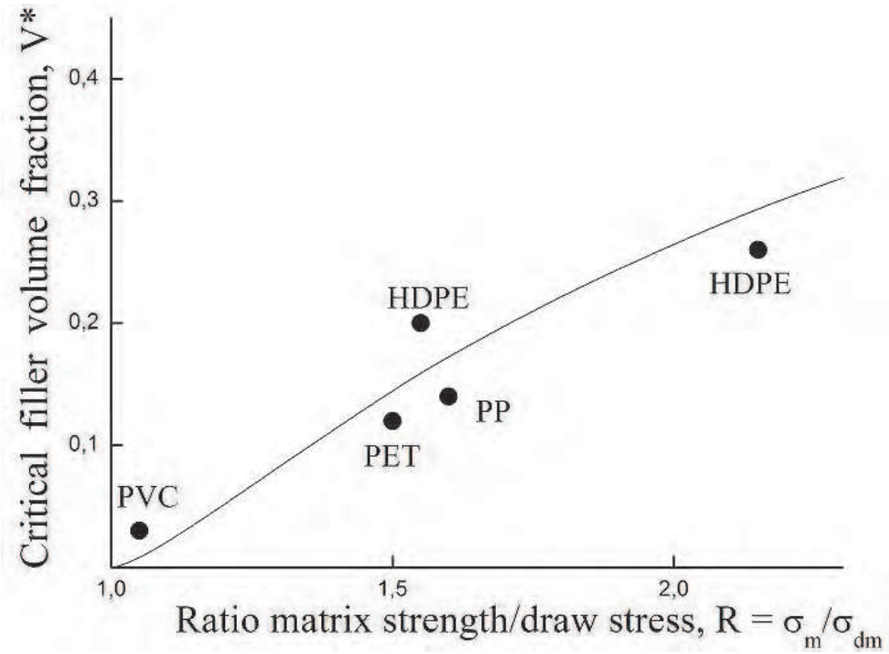

Fig. 16. The embrittlement filler content V* for well-bonded particles plotted against the ratio of the strength to the draw stress of unfilled matrix, $R = \sigma_m/\sigma_{dm}$. The points correspond to PVC, PET, PP and HDPE filled by particles with two different diameters, 8 and 25 μm.

6.2.1 $\sigma_m < \sigma_y$. Transition to brittle fracture

At week adhesion the draw stress corresponds to the lower border of the fork in Fig. 13, and the coefficient α in equation (5) is equal to 1 [7]. The critical filler content of the transition from neck propagation to brittle fracture is determined from criterion (1) and equations (2) and (5) at α = 1 [17]:

$$V^* = \frac{\beta^3 R^3}{27}[1 - 2\cos(\frac{\alpha}{3} + \frac{\pi}{3})]^3, \quad (8)$$

where β=1.21; $\alpha = \arccos[1 - \frac{27(R-1)}{2\beta^3 R^3}]$; $R = \sigma_m/\sigma_{dm}$; σ_m – strength and σ_{dm} – draw stress of the unfilled matrix.

Fig. 17 shows the embrittlement filler content V* plotted against the ratio of the strength to the draw stress of the matrix, σ_m/σ_{dm}. The critical filler content is determined by the matrix ability to strain-harden, similarly to the case of week adhesion. The critical filler content at good adhesion is higher than for well-bonded particles.

6.2.2 $\sigma_m > \sigma_y$. Transition to uniform yielding

Fig. 18 shows schematically the composite yield stress, strength and the draw stress plotted against the filler content, V_f. The strength, yield stress and the draw stress were calculated

with equations (2), (5) and (6). If the matrix strength is higher than its yield stress, the composite strength is higher than its yield stress at any filler content. At low filler contents the draw stress is lower than the yield stress and the strength of filled polymer. Hence, the neck propagates through the specimen, and filler does not change the deformation mode of the polymer. In contrast, at V>V** the yield stress is lower than the draw stress, and the yielding of the composite is uniform. Thus, fillers initiate transition from neck propagation to uniform yielding instead of brittle fracture [17]. This is a ductile to ductile transition allowing avoid the embrittlement of the composite. This behavior was observed in PP filled with $Al(OH)_3$ particles and glass spheres coated with release agent [18].
The criterion of the transition from neck propagation to uniform yielding is calculated from equation:

$$\sigma_d = \sigma_y \tag{9}$$

where σ_d and σ_y are the draw stress and the yield stress of filled polymer. Solution of equations (5), (6) and (9) gives the critical filler content V** of the transition from neck propagation to uniform yielding [17]:

$$V^{**} = \frac{\beta^3 R_1^{\,3}}{27}\left(1 - 2\cos\left(\frac{\alpha}{3} + \frac{\pi}{3}\right)\right)^3, \tag{10}$$

where β=1.21; $\alpha = \arccos\left(1 - \frac{27(R_1 - 1)}{2\beta^3 R_1^{\,3}}\right)$; $R_1 = \frac{\sigma_{ym}}{\sigma_{dm}}$, β=1,21; σ_{ym} – the yield stress and σ_{dm} – the draw stress of the matrix.
The critical filler concentration of the ductile to ductile transition is determined by the ratio of the yield stress to the draw stress of the unfilled matrix R_1. The ratio R_1 defines the height of the yield tooth. If the yield tooth is not high, R_1 value is close to 1. In this case the neck transition zone is not sharp. Therefore if the neck is not obvious transition occurs at a relatively low particle concentration. An increase in the yield tooth altitude results in an increase in R_1. Therefore to prevent embrittlement of filled composites the matrix should meet the following conditions: 1) the matrix strength should exceed the yield stress ($\sigma_m > \sigma_{ym}$) and 2) the yield point is not high.
Thus, fracture mode depends on matrix properties, particle content and their adhesion to the polymer matrix. Low amounts of filler do not change the fracture mode of a polymer. An increase in filler content leads to a transition in fracture mode. Usually this is the transition from ductile necking to brittle fracture. However, if the adhesion is weak and the strength is higher than the yield stress, the transition may be ductile-to-ductile from neck propagation to uniform yielding [17, 18].
Thus, the behavior of filled polymers depends on the matrix parameters which are not important for unfilled polymers. For example, the ratio of the strength to the draw stress and the ratio of the yield stress to the draw stress and even the yield point height.

6.3 Large particles

Fig. 19 shows a fracture strain of filled HDPE plotted against particle diameter D [19]. This dependence has maximum at the particle diameter of 10 μm. The decrease in fracture strain

with an increase in the particle diameter is explained by initiation of cracks by the large particles.

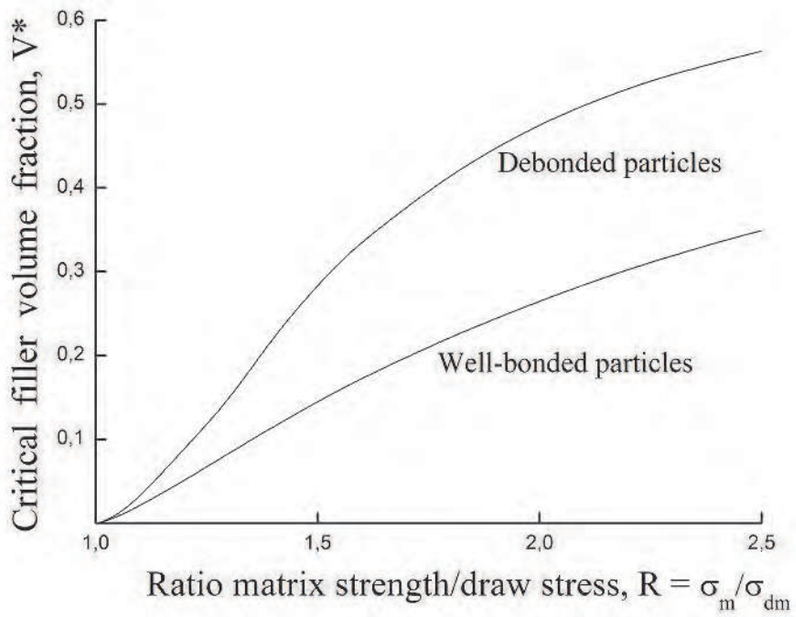

Fig. 17. The theoretical embrittlement filler content V* for well-bonded and debonded particles plotted against the ratio of the strength to the draw stress of unfilled matrix, R = σ_m/σ_{dm}. The curves were calculated with equations (7) and (8).

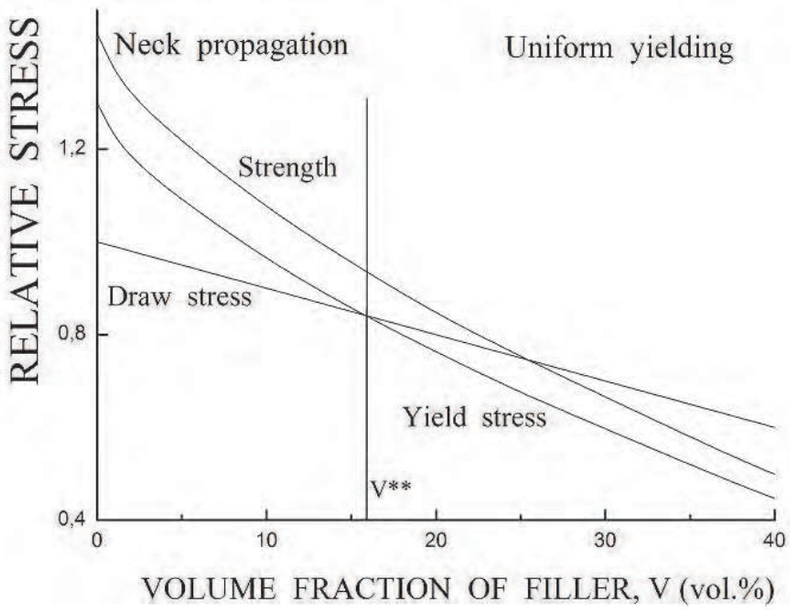

Fig. 18. Schematical drawing of the composite strength, draw stress and yield stress of filled polymer plotted against the filler content, V. V** - the critical filler content of the transition from neck propagation to uniform yielding [17].

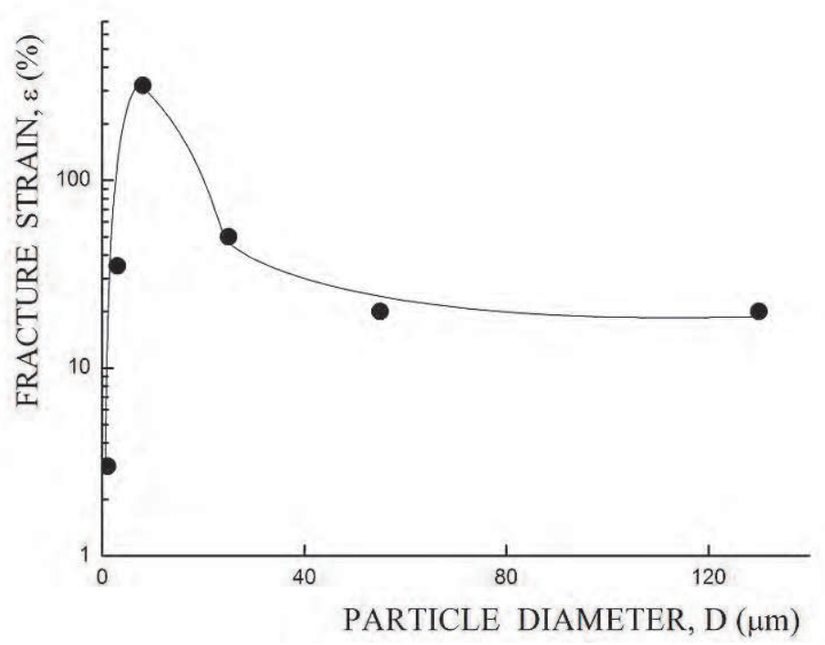

Fig. 19. Fracture strain of HDPE filled by rigid inorganic particles plotted against particle diameter, D [19].

Fig. 20 shows SEM images of fractured sample of HDPE filled by grinded rubber particles. Two types of pores in the composite are observed: large diamond pores (Fig. 20a) and small oval-shaped pores (Fig. 20b) [19]. Diamond pores appear only near large particles and oval pores near the small ones. Diamond pores are growing microcracks leading to material fracture. Pores of both types initiate as a result of particles debonding from the matrix.

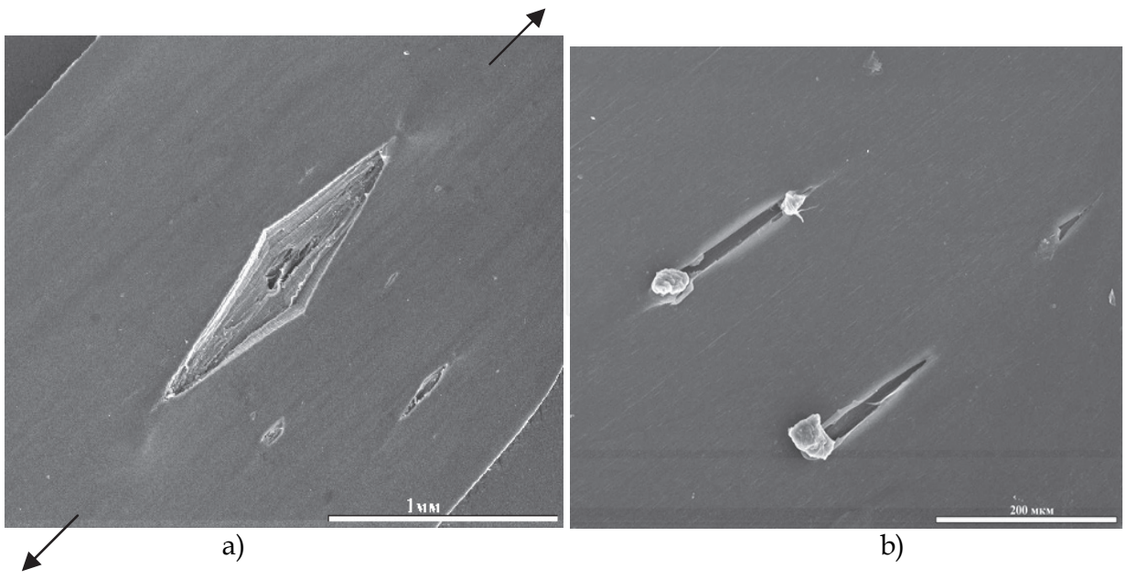

a) b)

Fig. 20. (a) - SEM image of diamond pores appearing near large grinded rubber particles in filled HDPE. (b) - SEM image of oval pores appearing near small grinded rubber particles. Arrows show the elongation direction.

Initiation of pores is schematically illustrated in Fig. 21. Oval pores originate near small particles (a); at tension they elongate but remain oval until fracture. Diamond pores form near large particles (c). An intermediate case is presented by an oval pore transforming in a diamond one in tension. Consequently, use of too large particles is undesirable. Large particles initiate appearance of diamond pores and premature fracture of a composite.

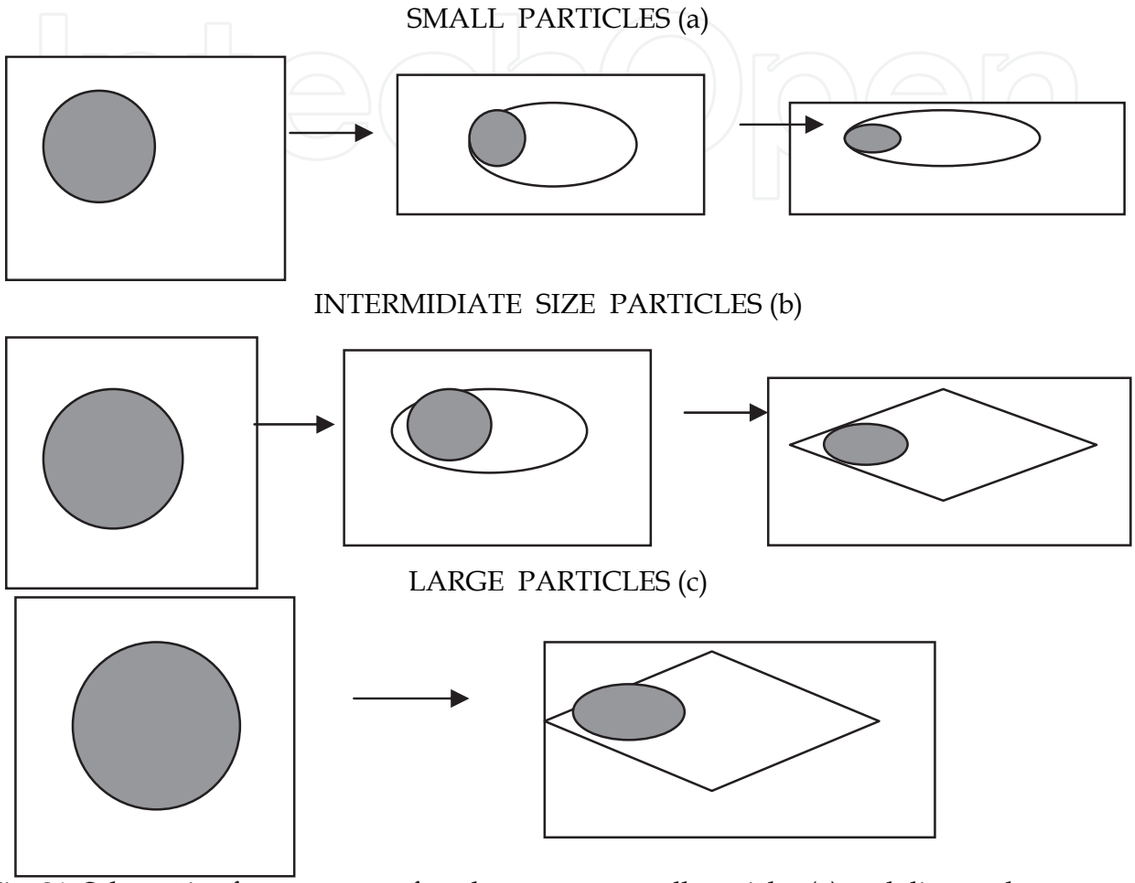

Fig. 21. Schematic of appearance of oval pores near small particles (a) and diamond pores near intermediate size (b) and large particles (c).

Behavior of a pore resembles a crack tip in a notched material. At small elongations the crack is blunted and its tip is round in shape (Fig. 22). Tension causes a gradual opening of the crack. At a certain point the geometry of its tip changes from rounded to V-shaped and the crack starts to grow. At further tension the size of the wedge grows through the sample. The wedge resembles a half of diamond pore.

The crack growth starts when its opening reaches a critical value of the crack opening δ_c [19]. Similarly an oval pore transforms into a diamond-shaped one when its opening reaches a critical value δ_c. Let us consider a pore initiated at elongation of a spherical particle with diameter D. Its length is $L = \lambda D$ (Fig. 22) and elongation is equal to the difference between the current length and initial size:

$$\delta = (\lambda - 1)\, D, \tag{11}$$

where λ is degree of the polymer matrix stretching.

Transformation of oval pore into a diamond one is described by the equation $\delta = \delta_c$, and the diamond pores appear only if the diameter of particles exceeds the critical value D*:

$$D^* = \delta_c/(\lambda - 1) \tag{12}$$

Equation (12) determines the elongation degree leading to initiation of diamond pores:

$$\lambda = \frac{\delta_c}{D} + 1 \tag{13}$$

Equation (13) determines transformation of oval pore into a diamond pore and the onset of fracture. The critical elongation is inversely proportional to the particle size. If the critical elongation λ is lower than the matrix elongation in the neck λ_d fracture is observed during the neck formation, and the composite is quasi-brittle. Therefore the critical particle size is

$$D^* = \delta_c/(\lambda_d - 1). \tag{14}$$

Fig. 23 shows that equation (14) quite accurately describes the critical diameter of particles initiating diamond pores. Large particles with the diameter exceeding D* should not be used in filled composites. Such particles initiate appearance of diamond pores and fracture of composite. The fracture toughness G_{Ic} is related with the critical crack opening δ_c by equation $G_{Ic} = \sigma_y\delta_c$, and (14) may be written:

$$D^* = \frac{G_{Ic}}{\sigma_y(\lambda_d - 1)} \tag{15}$$

where G_{Ic} is the fracture toughness and σ_y is the yield stress of the unfilled matrix. As shown in the previous sections, embrittlement is not typical for polymers deforming without necking. The effective method of suppressing necking is orientation of a polymer and, particularly, its rolling.

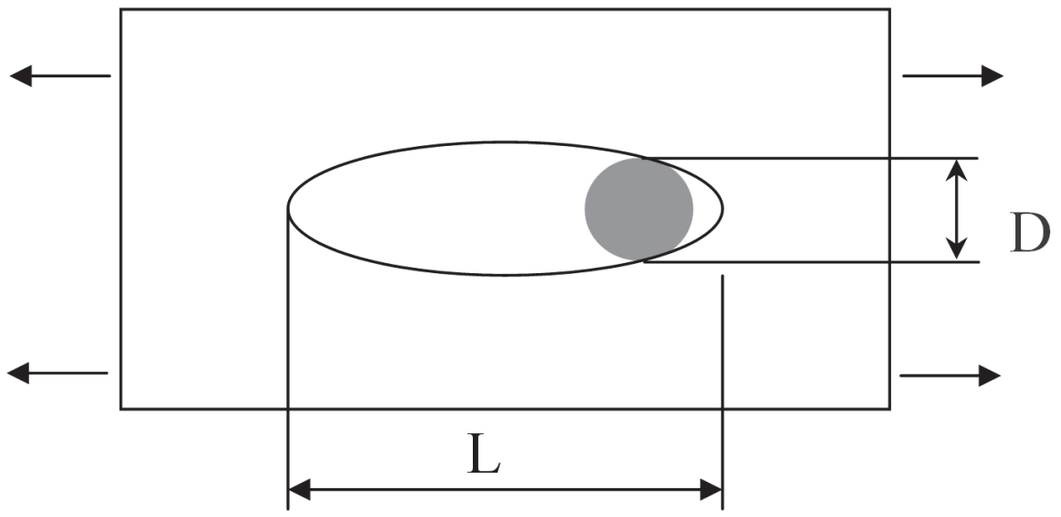

Fig. 22. Schematical drawing of oval pore appearing near a small particle (see Fig. 21a).

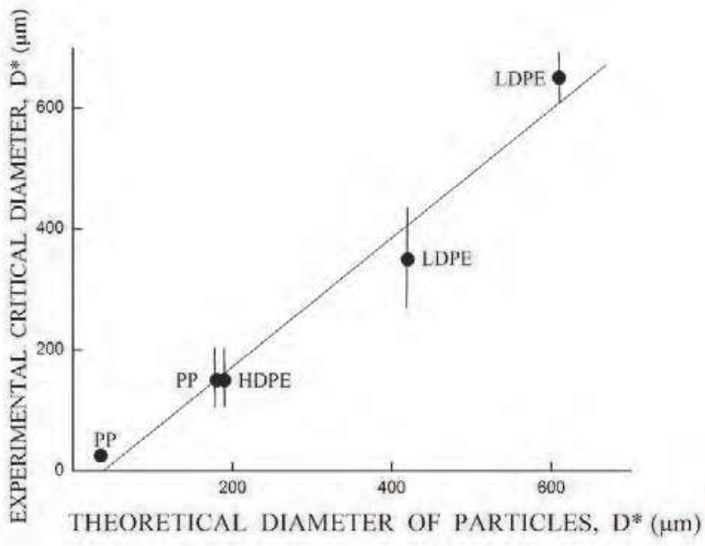

Fig. 23. Correlation between the experimental critical diameter of particles and theoretical values estimated with equation (15). Data are presented for HDPE, two types of LDPE and two types of PP [19].

7. Rolling

Fig. 24 shows typical engineering stress σ - strain ε curves for unoriented and rolled PET [20]. The increase in elongation degree after rolling leads to an increase in the ratio of the strength to draw stress. In addition, it suppresses necking and at the rolling degree λ = 1.9 the neck does not appear in the unfilled polymer. According to the above data, in this case brittle fracture of filled composite should not be observed and rolling suppresses embrittlement of filled polymers.

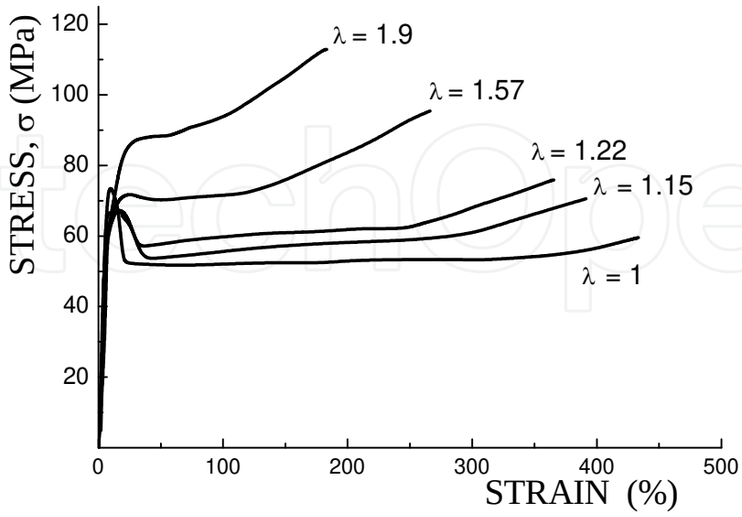

Fig. 24. Typical engineering stress σ versus strain ε curves of unoriented (λ=1) and rolled PET at rolling ratios λ=1.15; 1.22; 1.57 and 1.9. λ is equal to ratio of the sample length after rolling to its initial length.

Fig. 25 shows typical engineering stress σ - strain ε curves for unoriented and rolled PP filled with grinded rubber particles. An increase in rolling degree suppresses necking. The unoriented composite under tensile load is brittle (Fig. 25a) due to crazing of PP near large rubber particles. In contrast, rolled composites are ductile (Fig. 25b). At the rolling degree λ = 2.1 PP yields uniformely without necking. In addition, after rolling the crazes do not appear and filled composite is ductile. Hence, rolling effectively suppresses brittle fracture of filled polymers. Particularly, PP behaviour is ductile and crazes do not appear even at temperature -40°C [21, 22].

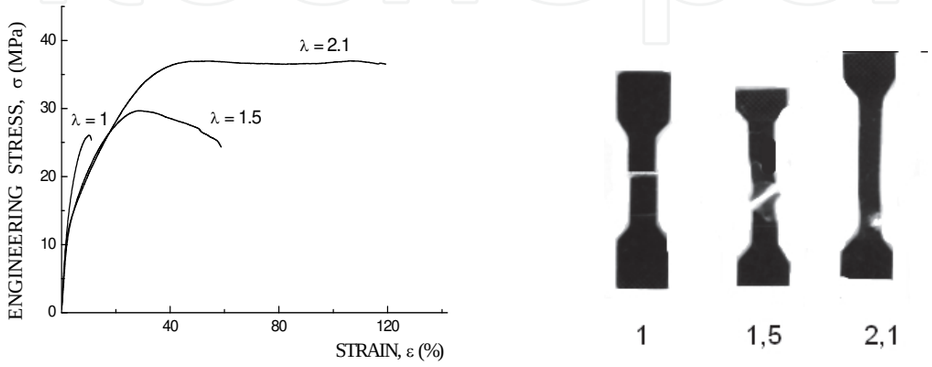

(a) (b)

Fig. 25. Typical engineering stress σ versus strain ε curves of PP filled with 8 vol.% of rubber particles at rolling ratios λ = 1 (unoriented), λ = 1.5 and 2.1. (b) – fractured samples.

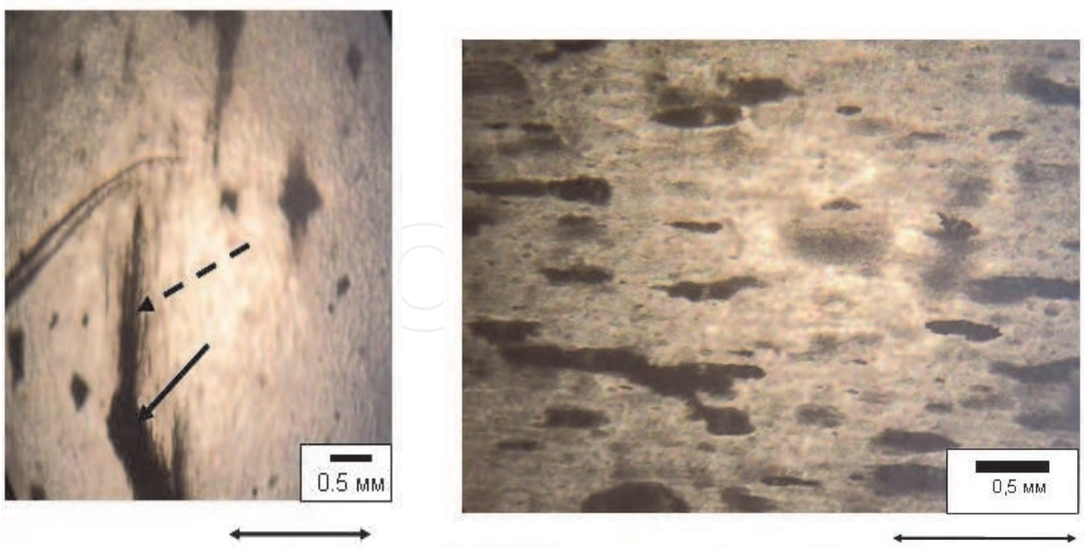

(a) (b)

Fig. 25. (a) – Crazes appearing near large rubber particles in unrolled PP under tension. (b) – Uniform deformation of PP filled with rubber particles after rolling to λ = 1.9. Arrows show the rolling elongation direction.

Fig. 26 shows engineering yield stress, draw stress and strength of PP plotted against the rolling ratio λ. At low rolling ratio λ the yield stress slightly decreases due to strain softening of the polymer. In addition, the difference between the yield stress and the draw stress decreases. Hence, rolling suppresses necking of the polymer. As a result, rolling allows avoid brittle fracture of filled polymer.

Fig. 27 illustrates the effect of rolling on the critical crack tip opening δ_c of HDPE. The critical crack tip opening δ_c sharply increases after rolling. Hence, rolling improves sensitivity of polymers to defects and, particularly, to filler particles. This also prevents brittle fracture of rolled composites.

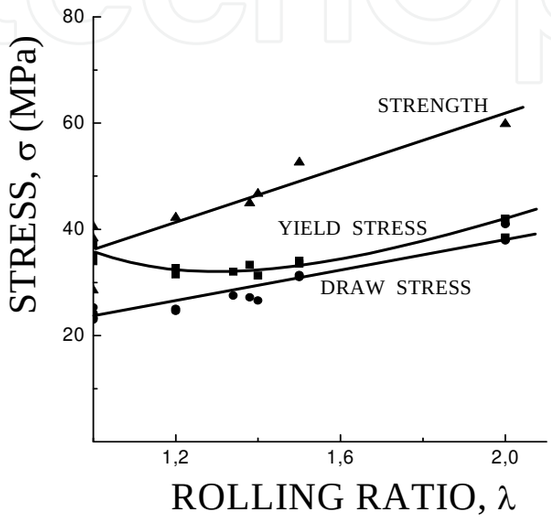

Fig. 26. Engineering yield stress, draw stress and strength of unfilled PET plotted against the rolling ratio λ [20].

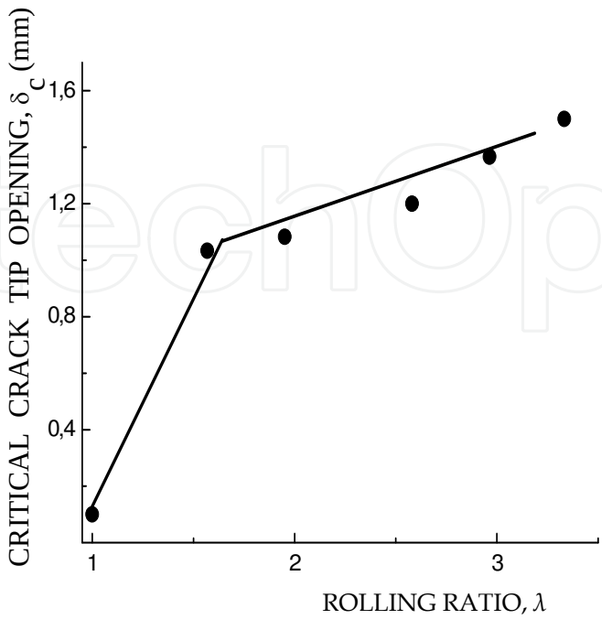

Fig. 27. Critical crack tip opening δ_c of HDPE plotted against the rolling ratio λ.

8. Conclusions

The main disadvantage of filled thermoplastic polymers is their brittle fracture. However, if unfilled polymer yields uniformly without necking, (PTFE, SHMWPE) composite remains ductile up to very high filler contents. Neck does not appear in polymers with very high molecular weight. Unfortunately, viscosity of these polymers is too high even at elevated temperatures, and they cannot be filled with particles by traditional liquid technologies.

The alternative method of necking suppression is orientation of polymer. Rolling is effective method of orientation of filled polymers. It allows avoid fracture during orientation, suppresses necking, improves ability to strain-hardening and leads to an increase in critical crack tip opening of polymer. As a result, rolled composites are ductile.

It is well known that orientation improves tensile strength and Young modulus of a polymer. In addition, it suppresses brittle fracture of unfilled and especially filled composites. Particularly, it suppresses crazing of polymers and composites.

The effect of particle size on fracture of particle filled composite is considered. Too large particles initiate appearance of diamond cracks and fracture of filled polymer. The critical particle size is determined by the critical crack tip opening or fracture toughness of the polymer matrix.

9. References

[1] Mathews F.L., Rawlings R.D. Composite materials: Engineering and science, Woodhead Publishing Limited, Cambridge, England (1999).
[2] Ashby M.F., Jones D.R.H., Engineering Materials, Elsevier Ltd. (2006).
[3] Tochin V.A., Shchupak E.N., Tumanov V.V., Kulachinskaya O.B., and Gai M.I., Mekh. Kompoz. Mater., 1984, p. 635.
[4] Berlin A.A., Topolkaraev V.A., Bazhenov S.L. Physical Aspects of Fracture and Deformation, Leningrad: Fizikotekh. Inst., 1987.
[5] Bazhenov S., Li J.X., Hiltner A., Baer E. J. Appl. Polym. Sci., 1994, 52, 243.
[6] Dubnikova I.L., Topolkaraev, V.A., Paramzina, T.V., and Diachkovskii, F.S., Visokomol. Soedin. 1, A32 (1990), 841.
[7] Bazhenov S.L. Fillers: their effect on the failure modes of plastics. // Plastics Additives. London, Chapmen and Hall. (1998). P.252.
[8] Bazhenov S.L., Grinev V.G., Kudinova O.I., Novokshonova L.A. Visokomol. Soedin. A52, 2010, p. 833.
[9] Novokshonova L.A., Meshkova I.N. Visokomol. Soedin. A36. 1994. P. 629.
[10] Grinev V.G., Kudinova O.I., Novokshonova L.A., Chmutin I.A., Shevchenko V.G. Visokomol. Soedin. A46. 2004. p. 1037.
[11] Novokshonova L.A., Meshkova I.N., Ushakova T.M., Grinev V.G., Ladigina T.A., Gultseva N.M., Kudinova O.I., De Boer S. J. Appl. Polym. Sci. 2003. V. 87. P. 577.
[12] Bazhenov S.L., Berlin A.A., Kulkov A.A., Ashmian V.G. Polymer Composite Materials. Intellect, 2010, p.347.
[13] Smith T.L. Trans. Soc. Reology. (1959), V.3, P.113.
[14] Nielsen L.E. J.Appl.Polym.Sci. 1966. V.10. P.97.
[15] Nicolais L., Narkis M. Polym. Eng.Sci. (1971), V.11, №3, P.194.
[16] Topolkaraev V.A., Tovmasian Y.M., Dubnikova I.L., Petrosian A.I., Meshkova I.N., Berlin A.A., Gomza Y.P., Shilov V.V. Composite Mechanics (1987), p.616.
[17] Bazhenov S., Polymer Engineering and Science, (1995), V.35, P.813.

[18] Dubnikova I.L., Topolkaraev V.A., Paramzina T.V., Gorokhova E.V., Diachkovsky F.S. Visokomol. Soedin. A32. 1990. p. 841.
[19] Bazhenov S.L., Serenko O.A., Berlin A.A., Dubnikova I.L., Berlin A.A. Doklady. 2003. V.393. p.336.
[20] Tunkin I.V., Bazhenov S.L., Efimov A.V., Kechekian A.S., Timan S.A. Visokomol. Soedin. A53, 2011 (to be published).
[21] Lin, Y. J.; Dias, P.; Chen, H. Y.; Hiltner, A.; Baer, E. Polymer, 49 (2008), 2578.
[22] Yang Y., Ponting M., Thompson G., Hiltner A. Baer E., J. Appl. Polymer Science (2011).

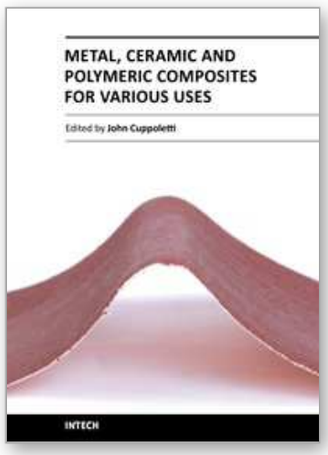

Metal, Ceramic and Polymeric Composites for Various Uses
Edited by Dr. John Cuppoletti

ISBN 978-953-307-353-8
Hard cover, 684 pages
Publisher InTech
Published online 20, July, 2011
Published in print edition July, 2011

Composite materials, often shortened to composites, are engineered or naturally occurring materials made from two or more constituent materials with significantly different physical or chemical properties which remain separate and distinct at the macroscopic or microscopic scale within the finished structure. The aim of this book is to provide comprehensive reference and text on composite materials and structures. This book will cover aspects of design, production, manufacturing, exploitation and maintenance of composite materials. The scope of the book covers scientific, technological and practical concepts concerning research, development and realization of composites.

How to reference
In order to correctly reference this scholarly work, feel free to copy and paste the following:

Sergey Bazhenov (2011). Mechanical Behavior of Filled Thermoplastic Polymers, Metal, Ceramic and Polymeric Composites for Various Uses, Dr. John Cuppoletti (Ed.), ISBN: 978-953-307-353-8, InTech, Available from: http://www.intechopen.com/books/metal-ceramic-and-polymeric-composites-for-various-uses/mechanical-behavior-of-filled-thermoplastic-polymers

INTECH
open science | open minds

InTech Europe
University Campus STeP Ri
Slavka Krautzeka 83/A
51000 Rijeka, Croatia
Phone: +385 (51) 770 447
Fax: +385 (51) 686 166
www.intechopen.com

InTech China
Unit 405, Office Block, Hotel Equatorial Shanghai
No.65, Yan An Road (West), Shanghai, 200040, China
中国上海市延安西路65号上海国际贵都大饭店办公楼405单元
Phone: +86-21-62489820
Fax: +86-21-62489821

IntechOpen